RSC Advances

ROYAL SOCIETY OF CHEMISTRY

www.rsc.org/advances

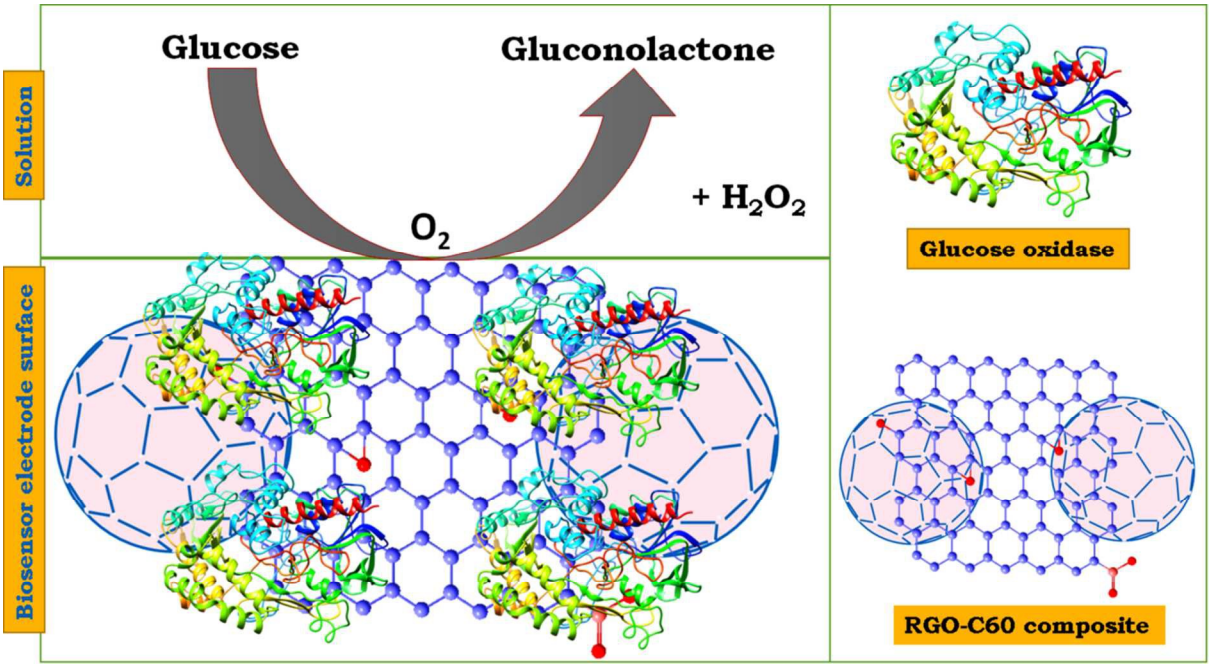

Schematic representation for the sensing of glucose at RGO–C60/GOx composite.

Journal Name

RSCPublishing

ARTICLE

Direct electrochemistry of glucose oxidase and sensing of glucose at glassy carbon electrode modified with reduced graphene oxide/fullerene-C60 nanocomposite

Cite this: DOI: 10.1039/xoxxoooooox

Received ooth January 2012,
Accepted ooth January 2012

DOI: 10.1039/xoxxoooooox

www.rsc.org/

Balamurugan Thirumalraj, [a‡] Selvakumar Palanisamy, [a‡] Shen-Ming Chen [a*] Cheng-Yu Yang, [a] Prakash Periakaruppan [b**] and Bih-Show Lou [c***]

In the present work, the glucose biosensor was fabricated based on the direct electrochemistry of glucose oxidase at glassy carbon modified with reduced graphene oxide (RGO) and fullerene-C60 (C60) composite. Reduced graphene oxide/fullerene (RGO–C60) composite was prepared by electrochemical reduction of graphene oxide (GO) and C60 composite at -1.4 V for 200 s in pH 5 solution; while the GO–C60 composite was prepared by a simple sonication of C60 in GO solution for 6 hours at 45˚C. A well-defined and enhanced reversible redox peak of GOx was observed at RGO–C60 composite compared to that of other modified electrodes. The heterogeneous electron transfer rate constant (Ks) and surface coverage concentration of GOx at RGO–C60/GOx modified electrode were calculated to be 2.92 s^{-1} and 1.19 x 10^{-10} mol cm^{-2}, respectively. Under optimum conditions, the amperometry response of the biosensor was linear against the concentration of glucose from 0.1 to 12.5 mM with a response time of 3 s. The limit of detection was estimated to be 35 µM based on S/N=3 with a high sensitivity of 55.97 $\mu AmM^{-1}cm^{-2}$. In addition, the fabricated biosensor showed good practical ability for the detection of glucose in the human blood serum samples.

1. Introduction

The direct electron transfer (DET) of redox active enzymes and proteins are continuously receiving much attention in different disciplines owing to their unique redox active electron transfer properties that are associated with redox active centre.[1, 2] The unique DET properties of the enzymes are more helpful for studying the key biological reactions and construction of biosensors and biofuel cells.[3] Among different redox active enzymes, glucose oxidase (GOx) is an ideal redox active enzyme for studying the electron transfer properties and has been widely used for construction glucose biosensors owing to its high specificity toward glucose.[4] The determination of glucose is always more important in the case of diabetes mellitus which is increasing rapidly.[5] As of 2013, 382 million people have been affected by diabetes worldwide as reported by International Diabetes Federation.[5] Hence, the fabrication of simple and sensitive glucose biosensors is necessary even though

tons of glucose biosensors already are available in the literature. The high specificity of GOx is more helpful for the construction of selective glucose biosensors.[6] However, the DET of GOx is often complicated or quite difficult at conventional electrodes due to the complex structure of GOx scaffold which directly prohibit the redox properties of the catalytic sites of GOx.[3] Over the past decades, the DET of GOx have successfully been realized and studied with the help of micro and/or nanomaterials modified electrodes, including the carbon materials, metal nanoparticles, metal oxides, conducting polymers, ionic liquids, etc.,[7–11]; Since the composites of nano and micro materials have shown an enhanced DET of GOx compared to individual one.

Reduced graphene oxide (RGO) is a carbon allotrope and the single atomic layer of carbon atoms that are arranged in a honeycomb lattice.[2] Since the discovery of RGO in 2004, it has been regularly used for different potential applications including energy conversion and storage, electronic devices, electrocatalysis, sensors and biosensors.[12, 13] However, the DET of GOx at pristine RGO surface is difficult due to the van der Waals force of attraction between each RGO sheets. Hence, the different approaches or micro or nanomaterials have been used with RGO to further enhance the electron transfer properties of GOx thus leading to the high sensitivity for the detection of glucose.[7] Recently, the composites of RGO with carbon nanomaterials, metal nanoparticles and metal oxides have been used as an electrode material for immobilization of GO, and they have shown an enhanced DET with better catalytic performance of GOx towards glucose compared to RGO.[14–16]

Fullerene C60 (C60) is one of the carbon allotropes and is made up of 60 closely packed carbon atoms into fused hexagons and pentagons without any edges.[17] Furthermore, it has been used as a promising electron transfer mediator for biomolecules and oxidase based amperometric biosensors and ECL biosensors.[19–21] In addition, it is reported earlier that C60 can be easily dispersed into the graphene oxide (GO) aqueous solution via covalent and non-covalent interactions.[20, 21] In addition, GO has been widely used for the preparation of hybrid carbon materials including carbon nanotubes and C60 owing to the presence of abundant oxygen functional groups.[21] In the present study, we have dispersed the C60 into the GO aqueous solution by simple sonication and the resulting GO–C60 composite has been electrochemically reduced to RGO–C60 composite by electrochemical method. Compared with other reduction methods, electrochemical method is more helpful to retain some of the oxygen functionalities on the carbon basal plane and the properties of RGO and C60. The reasons why we have chosen RGO¬C60 composite for biosensor are: i) the electrochemical behaviour of C60 is greatly improved in the presence of RGO, since pristine C60 has poor electrochemical behavior in aqueous solutions; ii) The electron transfer rate of enzyme towards the electrode surface is much improved at RGO–C60 composite when compared with pristine C60 and RGO, the amino terminal group of enzyme can be easily attracted by oxygen functional group of RGO and electron-releasing nature of enzymes and proteins can be easily attracted by conjugate π electron structure of C60 molecules.

Herein, we report the electrochemical preparation of the RGO–C60 composite by electrochemical reduction of GO–C60 composite at –1.2 V for 200 s in pH 5 solution. The GO–C60 composite was prepared by a simple sonication of C60 in GO aqueous solution for 6 hours at 45˚C. The fabricated RGO–C60 composite was further used as an immobilization matrix for GOx. The DET of GOx is greatly improved in presence of C60 with RGO. The GOx immobilized RGO–C60 composite electrode was subsequently used for the construction of glucose biosensor. The practicality of the biosensor in human blood serum samples have also been studied in detail.

2. Experimental

Materials and methods

Fullerene-C60 (99.5% purity) and graphite powder (98.0% purity) were obtained from Sigma–Aldrich. Glucose oxidase from *Aspergillus niger* was obtained from Sigma–Aldrich. Glucose, dopamine, ascorbic acid and uric acid were obtained from Aldrich. The supporting electrolyte 0.05 M pH 7 solution (PBS) was used for all electrochemical experiments and was prepared by using 0.05 M Na_2HPO_4 and NaH_2PO_4 solutions in doubly distilled water. All other chemicals used in this work were of analytical grade and all the solutions were prepared using doubly distilled water without any further purification. Human blood serum sample was collected from valley biomedical, Taiwan product & services, Inc. This study was reviewed and approved by the ethics committee of Chang-Gung memorial hospital through the contract no. IRB101-5042A3.

Cyclic voltammetry (CV) and amperometry *i-t* measurements were performed using the CHI 1205b and CHI 750a electrochemical stations. The surface morphology studies were carried out JSM-6500F scanning electron microscope. Raman spectrum was recorded using a Raman spectrometer (Dong Woo 500i, Korea) equipped with a 50 × objective and a charge-coupled detector. Ultraviolet–visible (UV-Vis) absorption spectra were obtained using a Hitachi U-3300 UV spectrophotometer. A conventional three-electrode system consisting of modified glassy carbon electrode (electrochemically active surface area = 0.12 cm^2) as a working electrode, an external saturated Ag/AgCl as a reference electrode and a platinum wire as the auxiliary electrode was used. Amperometric *i–t* measurements were performed using a PRDE-3A (AS distributed by BAS Inc. Japan) rotating ring disc electrode apparatus with an electrochemically working surface area of 0.033 cm^2. The electrochemically active surface area (EASA) of the GCE and RDE was calculated by CV according to our previous reported method.[22]

Preparation of RGO–C60 composite

GO was synthesized from natural graphite by using the Hummers' method as reported previously.[23] The GO aqueous solution was prepared by dispersing the GO (2 mg mL^{-1}) in water with the help of ultrasonication. In order to prepare the GO–C60 composite, the C60 in toluene solution was added into the GO aqueous solution (1:2, V: V %) and ultrasonicated for 6 hours at 45˚C. After 6 hours of ultrasonication at 45˚C, the colour of GO solution changes from brown to dark brown indicates the formation of GO–C60 composite. Ultrasonicator DC150H (Taiwan Delta New Instrument Co. Ltd.) with operating frequency of 40 kHz and ultrasonic power output of 150 W has been used for sonication.

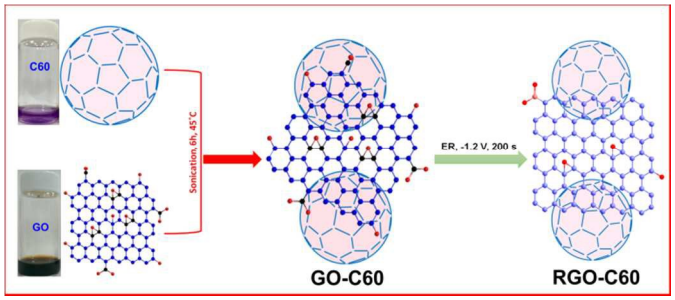

Fig. 1 A schematic representation for the preparation of RGO–C60 composite.

The effect of loading amount of GO and C60 on the biosensor response was optimized and the optimized conditions were used for the fabrication of the biosensor. The prepared GO–C60 composite was centrifuged at 2000 rpm to remove the unattached C60. About 8 µL of GO–C60 composite (optimum) was drop casted onto the pre-cleaned GCE and dried at room temperature. The GO–C60 composite modified GCE was transferred to N_2 saturated pH 5 solution and was electrochemically reduced to RGO–C60 composite by applying -1.4 V for 200. For comparison, the RGO modified GCE was prepared by electrochemical reduction of GO modified electrode without C60 by applying -1.4 V for 200 s. A schematic representation for the preparation of RGO–C60 composite is shown in Fig. 1.

Fabrication of RGO–C60/GOx biosensor

For the fabrication of biosensor, about 6 µL of GOx solution (5 mg mL^{-1} in PBS) was drop coated onto the RGO–C60 composite modified GCE. The fabricated biosensor was allowed to dry at room temperature and rinsed with deionized water before the electrochemical experiments. All electrochemical measurements were carried out at room temperature.

3. Results and Discussion

Characterization of RGO–C60 composite

Fig. 2 shows the SEM image of (A) GO and GO sonicated for 6 hr at 45˚C (inset), GO–C60 (B), C60 (inset of B), RGO (C) and RGO–C60 (D). The GO shows thin sheet morphology and RGO exhibits its typical crumble morphology associated with bundle of nanosheets. Fig. 2A inset clearly reveal that the surface morphology of GO did not changed upon sonication of GO for 6 hr at 45˚C.

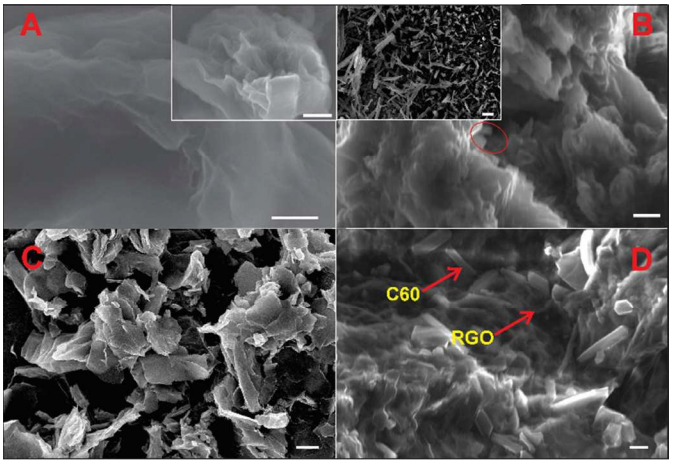

Fig. 2 SEM images of (A) GO and GO sonicated for 6 hr at 45˚C (inset), GO/C60 (B), RGO (C) and RGO/C60 (D). The inset of B shows the SEM image of C60. Scale bar = 1.5 µm.

On the other hand, the C60 reveals the typical rod-shape morphology of C60. The SEM image of GO–C60 composite clearly shows that the C60 rods are enfolded by GO sheets which indicate the formation of GO–C60 composite. While, the C60 rods are clearly seen on the RGO nanosheets and the morphology of RGO does not affect upon the electrochemical reduction of GO–C60 composite. The findings confirm the formation of RO–C60 composite.

The formation of RGO–C60 composite was further confirmed by Raman spectroscopy and UV-Vis spectroscopy. Raman spectroscopy is widely used for the confirmation of the electronic and lattice structures of carbon materials. Fig. 3A shows the Raman spectra of GO (a), C60 (b) and RGO–C60. It can be seen that C60 exhibits two distinct peaks at 1460 and 1680 cm^{-1}, which ascribed to the Ag and Hg mode of C60. While, the Raman spectrum of RGO–C60 composite shows D and G band at 1342 and 1596 cm^{-1}, which is related to the vibrations of sp^3 carbon atoms of disordered graphene nanosheets and vibrations of sp^2 carbon atom domains of graphite.[18] It should be noted that the Hg mode of C60 is not obviously visible on RGO–C60 composite, which maybe overlapping of Hg mode of C60 with the G-band of RGO. Similar results has been reported before for the presence of C60 with carbon nanomaterials.[18] In addition, the I_D/I_G ratio increase (I_D/I_G = 1.12) in RGO–C60 composite compared to GO (I_D/I_G = 0.91) which is due to the removal of oxygen functional groups in GO and formation of conjugated graphene network (sp^2 carbon) by electrochemical reduction process. The results confirm the formation of RGO–C60 composite.

The formation of GO–C60 composite is confirmed by UV-Vis spectroscopy and the results are shown in Fig. 3B. The C60 (curve a) shows a shoulder peak at 332 nm, which is assigned to π-π* electronic transitions of C60 molecules. The GO (curve b) exhibits an absorption maximum at 310 nm corresponding to n → π* transitions of C=O bonds.[25] On the other hand, RGO did not show the absorption peak at 310 nm, is due to the deoxygenation of the GO by electrochemical reduction processes. The GO–C60 composite shows absorption peaks at 331 nm and is related to the π-π stacking of C60 and GO. Since, the peak of C60 at 335 nm is a

vital indicator for the π–π interaction between the C60 and other organic compounds.[20] The RGO–C60 exhibits absorption peak at 332 nm and the peak of C60 at 310 nm disappear, which indicates that C60 molecule is assembled on graphene sheets through π-π interaction. The observed results are much similar to the previously reported RGO–C60 composite.[20, 26]

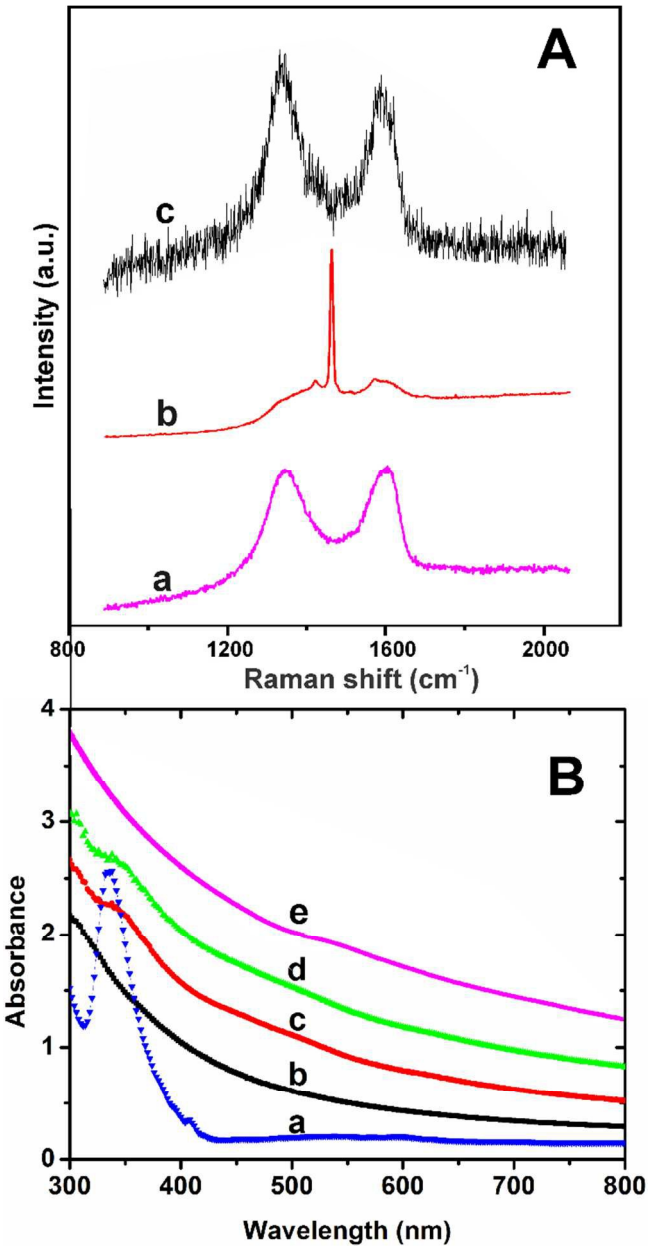

Fig. 3 A) Raman spectra of GO (a), C60 (b) and RGO–C60. B) UV-Vis spectra of C60 (a), GO (b), GO–C60 (c), RGO–C60 (d) and RGO (e).

Electrochemistry of GOx at different modified electrodes

The direct electrochemistry of GOx immobilized different modified electrodes was investigated using CV. Fig. 4 shows the CV response of GOx immobilized at C60 (a), GO–C60 (b), RGO (c) and RGO–C60 (d) modified GCEs in N_2 saturated PBS at a scan rate of 50 mV s^{-1} in the potential scanning from –0.7 to -0.1 V. A weak redox couple is observed at C60/GOx and the anodic peak potential (E_{pa}) and cathodic peak potential (E_{pc}) of redox couple is located at –0.396 and –0.432 V with a peak to peak separation (ΔE_p) of 36 mV, which is attributed to the direct electrochemical behavior of redox couple ($FAD/FADH_2$) in GOx.[27] The GO–C60/GOx modified GCE shows a pair of enhanced redox couple for GOx compared to that of C60. The E_{pa} and E_{pc} of redox couple is located at –0.405 and –0.396 V with a peak to peak separation (ΔE_p) of 31 mV, which is 5 mV lower than those observed at C60/GOx modified GCE. The GOx immobilized bare and GO modified GCEs does not show the redox couple at the same potential window (figure not shown), which indicates that C60 plays an important role in the DET of GOx towards the electrode surface.

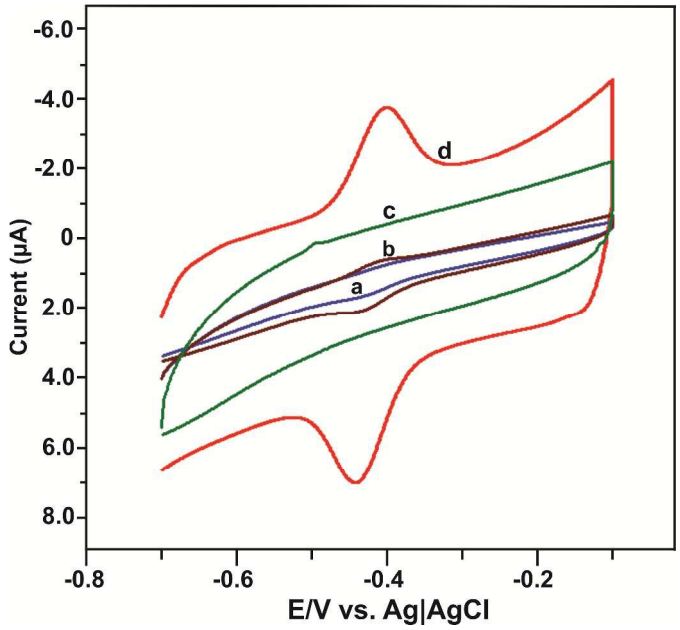

Fig. 4 A) CV response of C60/GOx (a), GO–C60/GOx (b), RGO (c) and RGO–C60/GOx modified electrode in N_2 saturated PBS at a scan rate of 50 mV s^{-1}.

On the other hand, RGO–C60/GOx modified electrode shows a well-defined redox peak for GOx and E_{pa} and E_{pc} of redox couple is observed at –0.439 and –0.405 V with a peak to peak separation (ΔE_p) of 34 mV. Furthermore, the I_{pa} and I_{pc} of redox couple is 5.6 folds higher than those observed at C60 and GO–C60 modified GCEs. RGO/GOx modified GCE shows less intense redox couple for GOx compared with other GOx immobilized modified GCEs. The results clearly indicate that RGO–C60 composite is favourable for DET between the electrode surface and the redox centers of GOx compared to other modified electrodes. The enhanced DET of GOx at RGO–C60 modified electrode is due to the combined unique properties of RGO and C60. Hence, RGO–C60/GOx modified electrode can be used as a sensitive biosensor for the detection of glucose.

Fig. S1A shows the effect of scan rate on the DET of GOx immobilized RGO–C60 modified electrode in PBS. It can be seen that the redox peak current of GOx increases with increasing the scan rates; while the E_{pa} and E_{pc} of redox couple is slightly shifted towards positive and negative direction upon increasing the scan rates from 10 to 200 mV s^{-1}. As shown in Fig. S1B, the anodic (I_{pa}) and cathodic peak current (I_{pc}) of redox couple have a linear dependence over the scan rates from 10 to 120 mV s^{-1} with the correlation coefficient of 0.9978 and 0.9983, respectively. The result suggests that the redox electrochemical behavior of GOx at RGO–C60 modified electrode is controlled by a surface-confined electrochemical process. The heterogeneous electron transfer rate constant (K_s) of GOx at RGO–C60/GOx modified electrode is calculated when the ΔE_p > 100 mV; since the number of electrons transferred in electrochemical reaction of GOx is 2. The value of K_s is calculated as 2.92 s^{-1} by using the following Laviron equation.[28]

$$Logk_s = \alpha Log(1-\alpha) + (1-\alpha)Log\alpha - Log\left(\frac{RT}{nFv}\right) - \alpha\frac{(1-\alpha)nF\Delta E_p}{2.3RT}$$

Where ΔE_p = peak-to-peak separation of the redox couple, n = 2, α is assumed to be 0.5 and all other symbols have usual meanings. The surface coverage concentration (Γ) of GOx at the modified electrode is calculated as 1.19 x 10^{-10} mol cm^{-2} using the following equation as reported early.[22]

$$\Gamma = Q/nFA$$

Where Q = total charge (5.7925 × 10^{-6} C), n = number of electrons involved in electrochemical reaction (n = 2), A= electrochemically active surface area of the electrode (0.12 cm^2) and all other symbols have usual meanings. The calculated value of *K*s is a bit higher than that of previously reported GOx immobilized composite modified electrodes indicating that the fast DET of GOx towards the electrode surface. In addition, the higher value of Γ indicates the high loading of GOx on RGO–C60 composite.[19, 29, 30]

The pH is an essential parameter to evaluate the DET of GOx at RGO–C60 modified electrode, since it greatly affects the DET behavior of GOx. Fig. S2A shows the CV response of GOx immobilized RGO–C60 modified electrode in N_2 saturated different pH solutions from 3 to 9 at a scan rate of 50 mV s^{-1}. It can be seen that a well-defined reversible redox peaks of GOx observed in each pH solution; the E_{pa} and E_{pc} of redox couple of GOx shift towards positive and negative direction upon decreasing and increasing the pH of the solution. As shown in Fig. S2B, the formal potential ($E^{o'}$, $E^{0'} = \frac{E_{pc} + E_{pa}}{2}$) of GOx has a linear dependence over the pH range from 3 to 9 with a slope of –51.9 mV/pH and a correlation coefficient of 0.9939. The observed slope value (−51.9 mV/pH) is close to the theoretical value of the Nernst equation for an equal number of proton and electron transfer reversible electrochemical process and it confirms that the DET of GOx involves equal number of protons (H^+) and electrons (e^-) transferred reaction. The DET of GOx can be written by the following Eqn. as reported previously.[31]

$$GOx\text{-}(FAD) + 2e^- + 2H^+ \leftrightarrow GOx\text{-}(FADH_2)$$

Amperometric determination of glucose

The electrocatalytic activity of the proposed biosensor towards glucose was evaluated by CV in oxygen saturated PBS at a scan rate of 50 mV s^{-1}. As shown in Fig. S3A, in absence of oxygen (curve a), a well-defined reversible redox couple of GOx is observed; while increase in cathodic peak current and decrease in anodic peak current is observed in the presence of oxygen (curve b). The result confirms that GOx is highly active in the presence of molecular oxygen. The reduction of molecular oxygen by of GOx can be written by following reaction.

$$GOx\text{-}(FAD) + 2e^- + 2H^+ \leftrightarrow GOx\text{-}(FADH_2) \quad (DET\ of\ GOx)$$

$$GOx\text{-}(FADH_2) + O_2 \rightarrow GOx\text{-}(FAD) + H_2O_2 \quad (O_2 reduction)$$

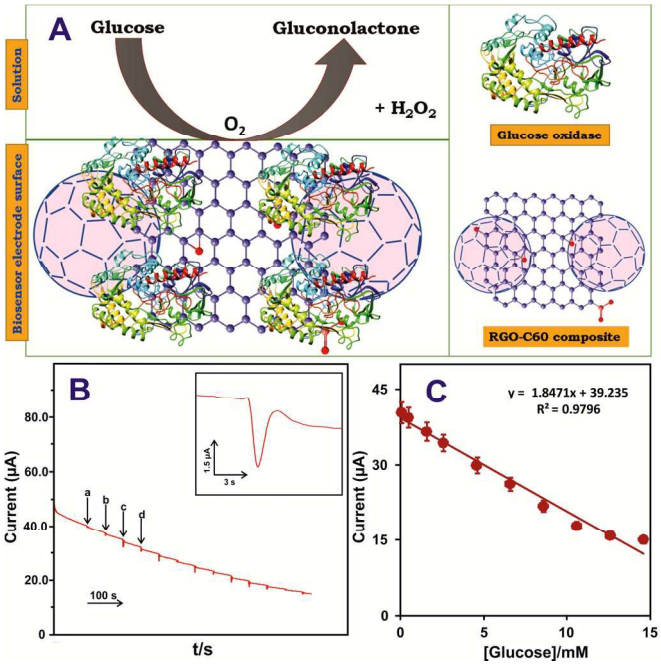

Fig. 5 A) Schematic representation for the sensing of glucose at RGO–C60/GOx composite. B) Amperometric *i-t* response obtained at RGO–C60/GOx biosensor for the addition of 0.1 mM (a), 0.5 mM (b) and 1 mM of glucose (c and d) up to 14.6 mM glucose into the constantly stirred oxygen saturated PBS; working potential is –0.42 V. Inset shows the enlarged view of amperometric response of the biosensor for addition of 1 mM glucose into the PBS. C) The calibration plot of [glucose] vs. amperometric current response.

Fig. S3B shows the CV response of RGO–C60/GOx modified electrode in the absence (a) and presence of different concentrations of glucose (b–g) in oxygen saturated PBS at a scan rate of 50 mV s^{-1}. It can be seen that the cathodic peak current decreases with increasing the concentration of glucose into the oxygen saturated PBS. The decrease in the cathodic peak current is due to the consumption of molecular oxygen and formation of H_2O_2. The high activity of GOx with molecular oxygen is resulting to the decrease of oxidized form of GOx on electrode surface. This is the reason why the addition of glucose restrained the electrocatalytic reaction and lead to the decrease of reduction current in the presence of oxygen. The similar phenomenon has been reported early in the literatures for oxidation of glucose by GOx in presence of oxygen.[31–33] The mechanism of glucose oxidation by GOx in presence of oxygen can be expressed by following equations, and the schematic representation of electro-oxidation of glucose in the presence of oxygen at RGO–C60/GOx composite is shown in Fig. 5A.

$$GOx\text{-}(FAD) + glucose \rightarrow Gluconolactone + GOx\text{-}(FADH_2)$$

$$GOx\text{-}(FADH_2) + O_2 \rightarrow GOx\text{-}(FAD) + H_2O_2$$

Amperometric *i-t* method was used for the determination of glucose using the proposed biosensor, since it is more sensitive method than that of other voltammetric methods. This is the reason why amperometric i-t method has been widely used for enzymatic biosensors. Fig. 5B shows the amperometric *i-t* response of RGO–C60/GOx modified electrode for the addition of different concentrations of glucose into the constantly stirred oxygen saturated PBS with the working potential of –0.42 V. A well-defined amperometric response is obtained for the each addition of 500 µM glucose into the PBS (inset). The amperometric reduction current decreases upon addition of further concentrations of glucose in to the

PBS and shows the response up to the addition of 14.6 mM glucose. The biosensor reaches its steady state current in 3 s. As shown in Fig. 5C, the amperometric i-t response current of the biosensor is linear against the concentration of glucose in the range of 0.1–12.5 mM. The limit of detection (LOD) was calculated as 35 μM based on *S/N*=3. The sensitivity is calculated from the slope of the calibration plot as 55.97 $\mu AmM^{-1} cm^{-2}$. The obtained linear response range of glucose is more suitable for the detection of glucose in human blood samples, since the normal glucose range in human blood in the range of 4.4 - 6.6 mM. The Michaelis–Menten constant (K_m) is calculated as 4.44 mM using a following Lineweaver–Burk equation.[34] The obtained K_m value is lower than those previously reported glucose biosensors, [33–36] which indicates the higher affinity of glucose towards biosensor electrode surface.

$$\frac{1}{I_{ss}} = \frac{1}{I_{max}} + \left(\frac{k_m}{I_{max}}\right)\left(\frac{1}{C_{glucose}}\right)$$

Where C = concentration of glucose in solution, I_{ss} = steady-state current, I_{max} = maximum current. K_m/I_{max} = slope of the plot of the reciprocals of I_{ss} vs. C and $1/I_{max}$ = intercept of the plot of the reciprocals of I_{ss} vs. C. It is necessary to compare the analytical performance of the proposed sensor with similar state of the art of other glucose biosensors. Hence, the comparison table is shown for the comparison of the analytical performance of the proposed glucose biosensor with previously reported glucose biosensors in Table ST1. It can be seen that the proposed biosensor shows higher sensitivity, low LOD along with wider linear response range to glucose compared to that of previously reported graphene based glucose biosensors and thus it can be used for electrochemical determination of glucose. [14, 25, 29, 31–33, 36, 37] The result confirms that the proposed biosensor has wider linear response range, better sensitivity with lower LOD. In addition, the high K_m value of the biosensor further confirms that it has high affinity towards glucose.

The selectivity of the proposed biosensor is always an important one especially for amperometric enzymatic biosensors; hence, the selectivity of the biosensor was investigated in the presence of potentially interfering compounds such as dopamine, ascorbic acid and uric acid. The selectivity of the biosensor was investigated using amperometry and shown in Fig. S4. The experimental conditions are similar as of Fig. 5B. It can be seen that the 5 mM addition of interfering compounds causes less interference effect on the modified electrode; while a sharp response for the addition of 1 mM glucose. The negative working potential is more beneficial for the less interference effect on the detection of glucose. The result confirms the appreciable selectivity of the biosensor towards the detection of glucose and can be used for the real time sensing of glucose in human serum samples without any interference effect.

The practical ability of the biosensor was evaluated for the detection of glucose in human blood serum samples using amperometry. The concentration of glucose was predetermined by a commercial detector and the appropriate concentration of blood serum was diluted with PBS for the real sample analysis. The experimental conditions are similar as of Fig. 5B. The recovery of glucose in human serum samples was calculated using the standard addition method[31], and the recovery of glucose is listed in Table ST2. It can be seen that the proposed sensor shows a satisfactory recovery towards glucose in human serum samples and the recovery was in the range of 97.5%. The satisfactory recovery of glucose in human serum samples authenticates the good practicality of the proposed biosensor.

The storage stability is of the biosensor was evaluated by CV and the cathodic response current of biosensor towards 1 mM glucose containing PBS was measured periodically and the results are shown in Fig. S5; the biosensor was stored in the refrigerator

when not in use. The biosensor retains its 90.9 % of its initial response towards glucose after stored in six days, which indicates the good storage stability of the proposed biosensor. The strong immobilization of the GOx in the composite matrix thus leads to the high activity of the biosensor. The repeatability and reproducibility of the sensor was evaluated using CV for the detection of 1 mM glucose. The three biosensors were prepared and used for the detection of glucose in the PBS and the relative standard deviation (RSD) of 3.9 % was observed. The RSD of 4.4 % was observed for the 8 measurements of the detection of 1 mM glucose containing PBS using a single biosensor. These results indicate a good precision and accuracy of the proposed sensor.

4. Conclusions

In conclusion, we have prepared the RGO–C60 composite by simple electrochemical reduction of GO–C60 composite. The DET of GOx greatly improves at RGO–C60 composite compared to other modified electrodes. The fabricated sensor shows good analytical features towards glucose such as wider response range, lower LOD, fast response time (3 s) along with high sensitivity. The good practicality of the biosensor in human serum samples confirms that it can be a suitable biosensor for real time sensing of glucose in blood serum samples. As a future perspective, the new novel composite possibly open a new way for the construction of different enzymatic biosensors.

Acknowledgments

This project was supported by the National Science Council and the Ministry of Education of Taiwan (Republic of China).

Notes and references

[a]Electroanalysis and Bioelectrochemistry Lab, Department of Chemical Engineering and Biotechnology, National Taipei University of Technology, No. 1, Section 3, Chung-Hsiao East Road, Taipei 106, Taiwan, ROC. E-mail: smchen78@ms15.hinet.net;
Fax: +886-2-27025238; Tel: +886-2-27017147.

[b]Department of Chemistry, Thiagarajar College, Madurai-625009, Tamilnadu, India.

[c]Chemistry Division, Center for General Education, Chang Gung University, Tao-Yuan, Taiwan.

‡ These authors contributed equally.

1. S. Afreen, K. Muthoosamy, S. Manickam and U. Hashim, *Biosens. Bioelectron.,* 2015, **63**, 354–364.
2. M.J. Allen, V.C. Tung and R.B. Kaner, *Chem. Rev.,* 2010, **110**, 132–145.
3. S. Shleev, J. Tkac, A. Christenson, T. Ruzgas, A.I. Yaropolov, J.W. Whittakerd and L. Gorton, *Biosens. Bioelectron.,* 2005, 20, 2517–2554.
4. Y.F. Bai, T.B. Xu, J.H.T. Luong and H.F. Cui, *Anal. Chem.,* 2014, **86**, 4910−4918.
5. Y. Shi and F.B. Hu, *The Lancet,* 2014, **383**, 1947–1948.
6. E.E. Ferapontova, S. Shleev, T. Ruzgas, L. Stoica, A. Christenson, J. Tkac, A.I. Yaropolov and L .Gorton, *Perspectives in Bioanalysis,* 2005, **1**, 517–598.
7. C. Chen, Q. Xie, D. Yang, H. Xiao, Y. Fu, Y. Tan and S. Yao, *RSC Adv.,* 2013, **3**, 4473–4491.
8. L. Chen, H. Xie and J. Li, *J. Solid State Electrochem.,* 2012, **16**, 3323–3329.
9. H.N. Choi, M.A. Kim and W.Y. Lee, *Anal. Chim. Acta,* 2005, **537**, 179–187.
10. Q. Xu, S.X. Gu, L. Jin, Y. Zhou, Z. Yang, W. Wang and X. Hu, *Sens. Actuators, B,* 2014, **190**, 562–569.
11. Q. Zhang, S. Wu, L. Zhang, J. Lu, F. Verproot, Y. Liu, Z. Xing, J. Li and X.M. Song,. *Biosens. Bioelectron.,* 2011, **26**, 2632–2637.
12. P. Avouris and C. Dimitrakopoulos, *Mater. Today,* 2012, **15**, 86–97.
13. J. Liu, Z. Liu, C.J. Barrow and W. Yang, *Anal. Chim. Acta,* 2015, **859**, 1–19.
14. V. Mani, B. Devadas and S.M. Chen, *Biosens. Bioelectron.,* 2013, **41**, 309–315.
15. C. Shan, H. Yang, D. Han, Q. Zhang, A. Ivaska and L. Niu, *Biosens. Bioelectron.,* 2010, **25**, 1070–1074.
16. S. Palanisamy, S. Ku and S.M. Chen, *Microchim. Acta*, 2013, **180**, 1037-1042.

17. C.K. Chua, Z. Sofer, P. Simek, O. Jankovsky, K. Klimova, S. Bakardjieva, S.H. Kuckova and M. Pumera, *ACS Nano*, 2015, **9**, 2548–2555.

18. B. Chai, T. Peng, X. Zhang, J. Mao, K. Li and Xungao Zhang, *Dalton Trans.,* 2013, **42**, 3402–3409.

19. C.Y. Deng, J.H. Chen, X.L. Chen, C.H. Xiao, L.H. Nie and S.Z. Yao, *Biosens. Bioelectron.,* 2008, **23**, 1272–1277.

20. Z. Hu, J. Li, Y. Huang, L. Chen and Z. Li, *RSC Adv.,* 2015, **5**, 654–664.

21. T. Gan, C. Hu and S. Hu, *Anal. Methods,* 2014, **6**, 9220–9227.

22. S. Palanisamy, C. Karuppiah, S.M. Chen, R. Emmanuel, P. Muthukrishnan and P. Prakash, *Sens. Actuators, B,* 2014, **202**, 177–184.

23. J. Guan, X. Chen, T. Wei, F. Liu, S. Wang, Q. Yang, Y. Lu and S. Yang,. *J. Mater. Chem. A*, 2015, **3**, 4139–4146.

24. S. Palanisamy, A.T.E. Vilian and S.M. Chen, *Int. J. Electrochem. Sci.,* 2012, **7**, 2153–2163.

25. S. Palanisamy, S. Cheemalapati and S. M. Chen, *Mater. Sci. Eng., C*, 2014, **34**, 207–213.

26. K. Zhang, Y. Zhang and S. Wang, *Sci. Rep.,* 2013, **3**, 3448.DOI: 10.1038/srep03448.

27. R. Zhao, X. Liu, J. Zhang, J. Zhu and D.K.Y. Wong, *Electrochim. Acta,* 2015, **163**, 64–70.

28. Y.D. Zhao, Y.H. Bi, W.D. Zhang and Q.M. Luo, *Talanta,* 2005, **65**, 489–494.

29.N. Hui, J.W. Cui, G.Q. Xu, S.B. Adeloju and Y.C. Wu, *Mater. Lett.,* 2013, **108**, 88–91.

30. A.G. Elie, C.H. Lei and R.H. Baughman, *Nanotechnology* 2002, **13**, 559–564.

31. B. Unnikrishnan, S. Palanisamy and S.M. Chen, *Biosens. Bioelectron.,* 2013, **39**, 70–75.

32. M. Shamsipur and M.A. Tabrizi, *Mater. Sci. Eng., C,* 2014, **45**, 103–108.

33. X. Kang, J. Wang, H. Wu, I.A. Aksay, J. Liu and Y. Lin, *Biosens. Bioelectron.,* 2009, **25**, 901–905.

34. Y. Huang, W. Zhang, H. Xiao, G. Li, *Biosens. Bioelectron.,* 2005, **21**, 817–821.

35. X. Liu, L. Shi, W. Niu, H. Li, G. Xu, *Biosens. Bioelectron.,* 2008, **23**, 1887–1890.

36. C. Ye, X. Zhong, R. Yuan and Y. Chai, *Sens. Actuators, B,* 2014, **199**, 101–107.

37. Z. Yanqin, Y. Wang, S. Yiliang, S. Xingcan and S. Zujin, *Chin. J. Chem.,* 2012, **30**, 1163–1167.

